Fast response and high sensitivity to microsaccades in a cascading-adaptation neural network with short-term synaptic depression

Wu-Jie Yuan,[1,2,*] Jian-Fang Zhou,[1] and Changsong Zhou[2,3,4,†]

[1]*College of Physics and Electronic Information, Huaibei Normal University, Huaibei 235000, China*

[2]*Department of Physics, Hong Kong Baptist University, Kowloon Tong, Hong Kong, China*

[3]*Centre for Nonlinear Studies, Institute of Computational and Theoretical Studies, Hong Kong Baptist University, Kowloon Tong, Hong Kong, China*

[4]*Research Centre, HKBU Institute of Research and Continuing Education, Virtual University Park Building, South Area Hi-tech Industrial Park, Shenzhen, China*

(Received 4 September 2015; revised manuscript received 26 February 2016; published 4 April 2016)

Microsaccades are very small eye movements during fixation. Experimentally, they have been found to play an important role in visual information processing. However, neural responses induced by microsaccades are not yet well understood and are rarely studied theoretically. Here we propose a network model with a cascading adaptation including both retinal adaptation and short-term depression (STD) at thalamocortical synapses. In the neural network model, we compare the microsaccade-induced neural responses in the presence of STD and those without STD. It is found that the cascading with STD can give rise to faster and sharper responses to microsaccades. Moreover, STD can enhance response effectiveness and sensitivity to microsaccadic spatiotemporal changes, suggesting improved detection of small eye movements (or moving visual objects). We also explore the mechanism of the response properties in the model. Our studies strongly indicate that STD plays an important role in neural responses to microsaccades. Our model considers simultaneously retinal adaptation and STD at thalamocortical synapses in the study of microsaccade-induced neural activity, and may be useful for further investigation of the functional roles of microsaccades in visual information processing.

DOI: 10.1103/PhysRevE.93.042302

I. INTRODUCTION

Microsaccades are involuntary, fast, and very small eye movements during fixation. Recently, the investigations of microsaccades have been mainly focused on experimental studies of their behavioral properties and functional roles [1,2]. However, neural responses induced by microsaccades are not yet well understood and have been rarely studied theoretically [3,4].

Experimentally, it has been found that microsaccades play an important functional role in counteracting visual fading during fixation [5,6]. Several studies have assumed that microsaccades refresh retinal images by moving the receptive fields of less adapted photoreceptors over stationary stimuli, thereby preventing perceptual fading [5,7]. Indeed, retinal adaptation has been extensively found in experiments [8–12]. According to the above assumption, retinal adaptation should affect the microsaccade-induced neural responses.

Short-term depression (STD) is a typical synaptic plasticity [13]. Recently, STD has been extensively found at thalamocortical synapses from the lateral geniculate nucleus (LGN) to the primary visual cortex (V1) *in vitro* [14,15] and *in vivo* [16] in cats. Previously, network models of V1 neurons with STD at thalamocortical synapses have been used to account for important response properties of cortical neurons [17–19]. Some other computational studies have also explored the impact of STD on network dynamics and found various rich dynamical properties [20–29], suggesting many important roles of STD in neural computations. Especially, our recent work proposed that STD at thalamocortical synapses could provide an alternative explanation for microsaccades in counteracting visual fading during fixation [30]. The adapted synapses subjected to STD lead to response depression in V1 during fixation; when microsaccades occur, the neural responses return owing to relative moving of the fixated dot to neurons with less adapted synapses. Our further simulations showed that this alternative STD model can reproduce several experimentally observed features in microsaccade-induced neural responses [30]. The model can produce several further predictions about the dependence of the responses on experimental parameters [31], such as stimulus brightness, microsaccade size, and so on.

However, this existing literature has not considered retinal adaptation in the study of the effect of STD. Actually, retinal adaptation is not exclusive with STD at thalamocortical synapses. When these two levels of adaptations are put into a cascading network, their interplay is expected to generate richer dynamics in V1 neurons. The neural activity in V1 is a crucial component for understanding visual information processing in the brain [32,33]. Since the thalamocortical synapses subjected to STD are directly linked to neurons in V1, STD is supposed to play an important role in microsaccade-induced responses of the V1 neurons together with the retinal adaptation. In this paper, we study the role of STD in the cascading-adaptation network, including simultaneously retinal adaptation and STD at thalamocortical synapses.

II. MODEL

According to visual pathway [34,35], a feed-forward network model with cascading adaptations is proposed in Fig. 1(a), including both the retinal adaptation and STD at

*yuanwj2005@163.com

†cszhou@hkbu.edu.hk

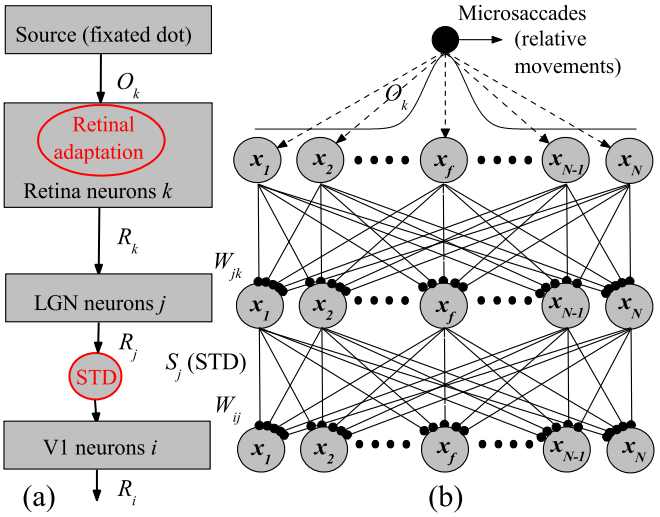

FIG. 1. The feed-forward cascading-adaptation network model including retinal adaptation and STD during fixation with microsaccades. (a) A schematic sketch of the visual pathway. The received optical strengths O_k from the fixated dot induce the firings in retina cells; the firings with rate R_k in the retina are directly projected to LGN, then the produced firings with rate R_j in LGN are straightly projected to V1, and finally the firings with rate R_i are generated in V1. (b) Illustration of the feed-forward network structure. There is the same number of N neurons in the retina, LGN, and V1. These neurons in the retina, LGN, and V1 are all labeled and arranged corresponding to the center positions x_k, x_j, and x_i of their receptive fields distributed uniformly in the ranges from $-L$ to L, respectively. x_f denotes the position of the fixated point. The retina cells are connected to LGN by neural synapses with linking weights W_{jk}. The LGN are then connected to V1 by thalamocortical synapses with linking weights W_{ij} and with synaptic strengths S_j, which are subjected to the modification by STD. The microsaccades during fixation can be regarded as instantaneous relative movements of the fixated dot. In order to eliminate the effect of boundaries due to limited network scale, periodic boundary conditions are applied to the three layers of the network (thus to the coupling between layers and the input curve O_k [i.e., $O(x_k)$], i.e., $O(x_k + 2Ln) = O(x_k)$ [if $(x_k + 2Ln) \notin [-L, L]$; n is an integer].

the thalamocortical synapses. The model is composed of excitatory neurons, described by membrane potential and firing rate. The firings with rate R_k in the retinal cell k are directly projected to the neuron j in LGN. Then, the firings with rate R_j in the neuron j are straightly projected to the neuron i in V1 by synapses with STD.

More details of the feed-forward network structure are shown in Fig. 1(b) and described in its caption. In visual systems, a neuron sees only a small portion of the visual field. This small area is called receptive field of the cell. Because of receptive fields (Gaussian filters) in retinal cells [36,37], the distribution of received optical strength O_k is assumed to be a Gaussian profile: $O_k = O(x_k) = A \exp^{-(x_k - x_f)^2/\sigma_1^2}$. Here A represents the amplitude of a visual input at the fixated-dot position x_f. σ_1 denotes the width of the tuning curve. The spatial connecting weights W_{jk} and W_{ij} caused by the receptive fields of LGN and V1 neurons follow Gaussian tuning curves [30,35]: $W_{jk} = \exp^{-(x_k - x_j)^2/\sigma_2^2}$ and $W_{ij} = \exp^{-(x_j - x_i)^2/\sigma_2^2}$, respectively. σ_2 of the Gaussian curves denotes the width of the connecting strength distributions. In principle, the projection widthes to LGN and to V1 could be different, but they do not change the results qualitatively. For simplicity, we ignore the time courses of microsaccades since microsaccades are very fast eye movements [1]. Thus it is assumed that a microsaccade with magnitude M happens instantaneously. Here, microsaccades can be regarded as instantaneous relative movements of the fixated dot over the retina with magnitude M, i.e., movements of the optical strength curve O_k evoked by the fixated dot.

In our model, we assume that the N neurons in the retina, LGN, and V1 are, respectively, spread uniformly in the ranges from $-L$ to L, which denote the physical positions of the centers of the receptive field of these neurons. Compared with the responsive region of neurons induced by the fixated dot, L should be large enough that the new place of fixated dot after a microsaccade is far from the boundary neurons. In order to limit the simulating time with reasonably finite L, but to eliminate the effect of boundary, we use periodic boundary conditions for the three layers. The received optical strength O_k is thus extended to a period boundary function with periodic value $2L$ [see the caption of Fig. 1(b)]. In this way, the value of L does not qualitatively change the results. Since microsaccades happen rather quickly, here they are modeled by instantaneous relative displacement M of the curve O_k on the one-dimensional straight direction of retinal neural positions. With suitable scale transformation, the size L and displacement M can be used to represent realistic range of microsaccades [1].

In the neural network, the dynamics of membrane potential V_j in the LGN neuron j is described by

$$\tau_m \frac{dV_j}{dt} = -V_j + \sum_{k=1}^{N} g W_{jk} R_k. \quad (1)$$

The parameter τ_m denotes the membrane time constant. g represents the maximal synaptic conductance. W_{jk} denotes the projection weight from the retinal cell k to the LGN neuron j. N is the number of neurons in retina. Each LGN neuron j integrates inputs coming from retinal cell k with firing rate R_k. Biologically, when the potential V_j reaches a threshold value, the neuron j emits a spike, and then the membrane potential is reset to a relatively low value. In order to avoid the short-time dynamics required to simulate spikes of the action potential and chemical synapses, we here adopt a firing rate model, which is much easier to simulate on a computer. The firing rate R_j of the neuron j is related to the membrane potential by the logistic function [38],

$$R_j = \frac{\alpha}{1 + e^{-\beta(V_j - \theta)}}, \quad (2)$$

where α, β, and θ are constants. α is the maximal rate, β is the steepness of the response function, and θ, the midpoint of the function, represents the effective firing threshold. The logistic function is often used in neural network models to introduce nonlinearity in neural rate responses, which can well approximate the dynamics of spiking neurons [38]. The logistic firing rate model provides an attractive approach for

studying large neural network because it can be simulated rapidly.

In addition, there is similar neural dynamics in the V1 neuron i to Eqs. (1) and (2) as follows:

$$\tau_m \frac{dV_i}{dt} = -V_i + \sum_{j=1}^{N} g W_{ij} S_j R_j \tag{3}$$

and

$$R_i = \frac{\alpha}{1 + e^{-\beta(V_i - \theta)}}, \tag{4}$$

where W_{ij} represents the linking weight from the LGN neuron j to the V1 neuron i, N is the number of neurons in LGN and S_j denotes the synaptic strength from neuron j to neurons in V1. In biological spiking neuron, the synaptic strength S_j is subjected to the following STD mechanism [13,19,39]:

$$\frac{dS_j}{dt} = \frac{1}{\tau_S}(1 - S_j) - (1 - f_S) S_j \sum_{\mu} \delta(t - t_\mu), \tag{5}$$

where t_μ is the time of the μth spike generated by neuron j and $\delta(t - t_\mu)$ is the Dirac δ function. The parameter f_S ($0.0 < f_S < 1.0$) determines the amount of depression at synapse j induced by each spike from neuron j. The parameter τ_S denotes the recovery time of the neuron transmitters from depletion. When the afferent neuron j fires a Poisson spike train at rate R_j, the synaptic strength will quickly decrease to the approximate steady state (SS) $S_j(\mathrm{SS}) = \frac{1}{1+(1-f_S)\tau_S R_j}$ for a high rate R_j [13,19]. For a very small firing rate R_j, the synaptic strength approximately maintains its original value 1. This depression model gives a good fit of experimental data [13]. To simplify calculation with the rate model, we transform Eq. (5) into the following equation with the firing rate R_j:

$$\frac{dS_j}{dt} = \frac{1}{\tau_S}(1 - S_j) - (1 - f_S) S_j R_j. \tag{6}$$

Obviously, the synaptic strength in Eq. (6) has the same solution of its steady state (SS),

$$S_j(\mathrm{SS}) = \frac{1}{1 + (1 - f_S)\tau_S R_j}, \tag{7}$$

as in Eq. (5) for a high firing rate R_j. In this way, we avoid direct simulations of the spike trains in the neuron j, which can reduce the amount of computation.

In the retina, neural responsive adaptation has been extensively found in experiments [40,41]. The adaptive response is mainly reflected in the output of retinal ganglion cells. It has been experimentally observed that the responses of retinal ganglion cells become weaker and weaker in the presence of sustained stimulus from light [42]. However, the retinal adaptation has not been successfully described by using a physiologically realistic model that can fit actual experimental data [43]. Based on the experimental observation of reduced responses [42], we here propose a phenomenological model for the retinal adaptation. Motivated by the mathematical description of the synaptic STD, the firing rate R_k in retinal cell k could be described by

$$R_k = r_k O_k, \tag{8}$$

where r_k is an adaptation factor of the neural response from the received optical strength O_k (coming from the fixated dot) to the firing rate R_k. The factor r_k denotes resources required for the response. Here, we suppose that the variation of the resources is similar to that of synaptic transmitter resources responsible for STD, which can be regarded as the interaction between two processes including activity-dependent depletion and slow replenishment after each firing spike of the presynaptic neuron [13,16,39]. Similar to the property of STD in Eq. (6), we can describe r_k by using the following adaptation scheme:

$$\frac{dr_k}{dt} = \frac{1}{\tau_r}(1 - r_k) - (1 - f_r) r_k O_k, \tag{9}$$

where τ_r and f_r denote constants with biophysical significance similar to τ_S and f_S in Eq. (6).

In the simulations, we take $N = 1000$ and $L = 10$. The other parameters in our model are given by $\tau_m = 30$ ms, $\sigma_1 = \sigma_2 = 1.5$, $\alpha = 200$, $\beta = 1$, $\theta = 6$, $A = 60$, $\tau_S = \tau_r = 200$ ms, and $f_S = f_r = 0.75$, except for special description for comparisons. The main results, however, do not sensitively depend on these parameters. Choosing different parameter values does not alter the qualitative results.

III. RESULTS

A. Fast and sharp response

By using the above network model, we compute V1 neural responses to microsaccades in the following simulations. In Fig. 2(a), we plot the V1 network-averaged firing rate $\langle R_i \rangle$ induced by fixation and successive microsaccades. Clearly, the neural activity begins to fade within several hundreds of milliseconds after the start of fixation in the absence of microsaccades. If a microsaccade occurs, the neural excitation

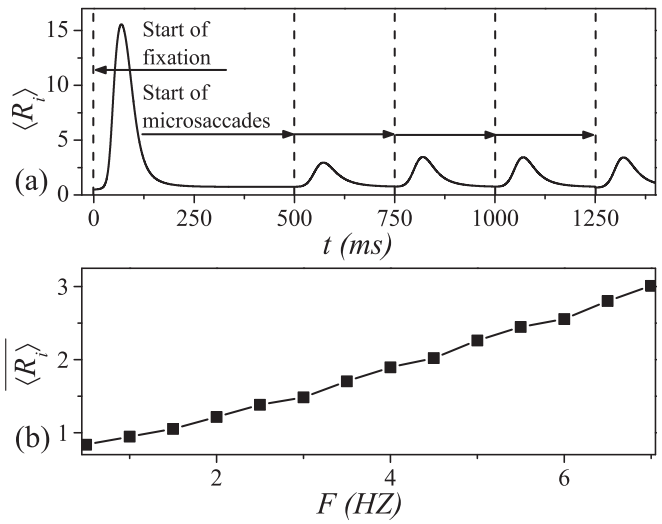

FIG. 2. Response in V1 to many microsaccades with frequency F. (a) The network-averaged firing rate $\langle R_i \rangle$ induced by periodic microsaccades with a frequency $F = 4$ Hz. (b) The time-averaged neural activity $\overline{\langle R_i \rangle}$ during the fixation lasting for $t = 100$ s with random microsaccades (in Poisson train) as a function of microsaccade frequency F. Here, the parameters are $g = 1.8$, $M = 2.2$.

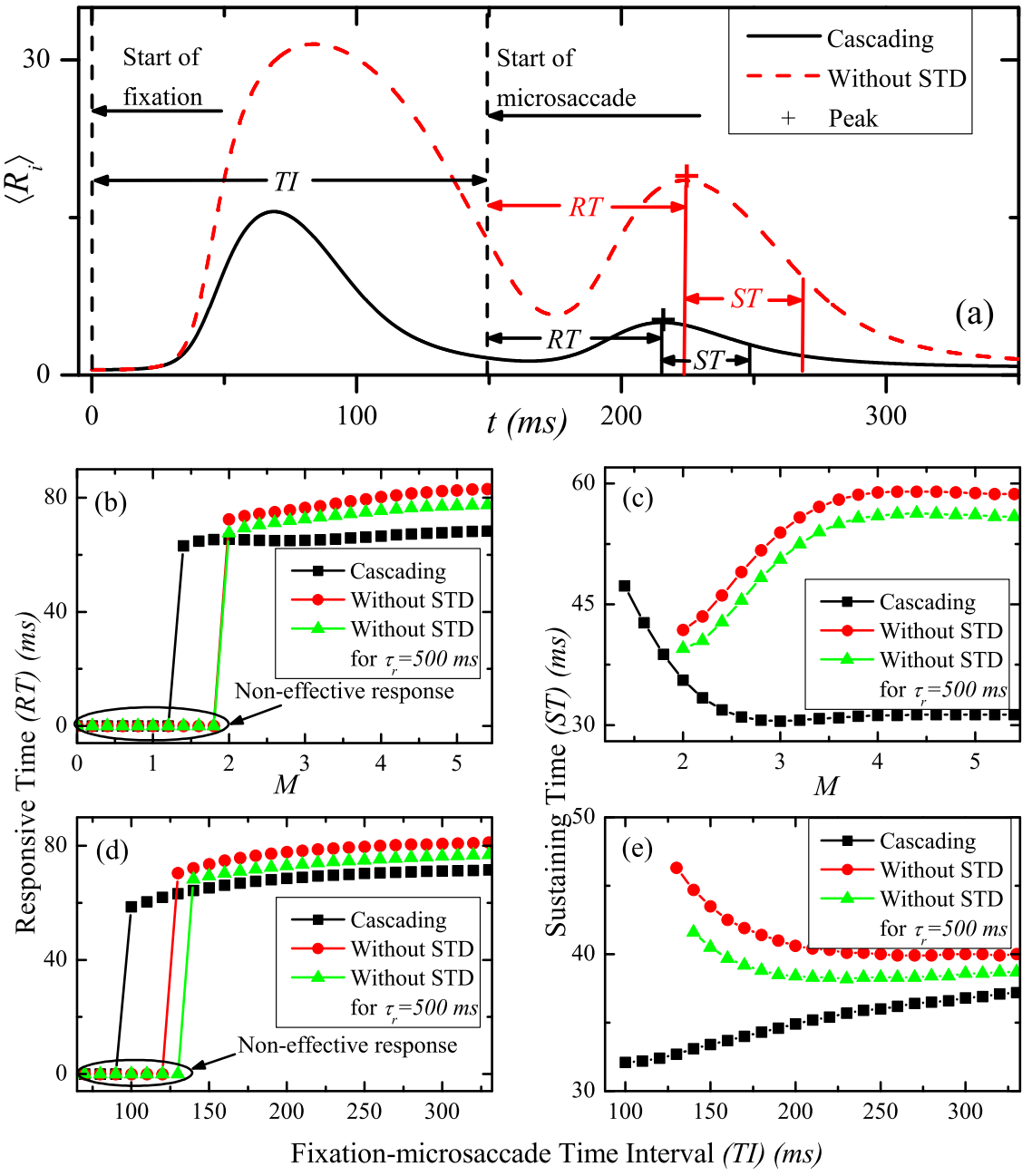

FIG. 3. Comparison of V1 response time scale induced by microsaccade in the cascading-adaptation network model and in the absence of STD. (a) The network-averaged firing rate $\langle R_i \rangle$ evoked by the fixation and a microsaccade which occurs at the time interval TI after the onset of the fixation. In (a), solid verticals denote response peaks and half-high values between peak and baseline. The response time RT [(b) and (d)] and the sustaining time ST [(c) and (e)] of the effective responsiveness as a function of the microsaccade magnitude M [(b) and (c)] and the fixation-microsaccade time interval TI [(d) and (e)]. In (b) and (d), zero response time denotes noneffective response, i.e., the nonoccurrence of the response peak after the microsaccade in (a). For further comparison, the response time and the sustaining time are given in (b)–(e) for the case without STD, but with a higher level of the retinal adaptation (by increasing the time scale τ_r to 500 ms, so that the retinal adaptation recovers more slowly). Here, we use $g = 1.8$, TI $= 150$ ms [(a)–(c)] and $M = 2.2$ [(a), (d), and (e)].

will return and persist for a few hundreds of milliseconds. The neural activity is sustained and does not fade away completely if there are more microsaccades with high enough frequency (e.g., $F = 4$ Hz), which is consistent with the fact that microsaccades occur a few (about 4) times per second [1]. As suggested in Ref. [30], the neural activity induced by microsaccades can provide a possible dynamical explanation for microsaccades' role in counteracting visual fading. Here, we calculate the time-averaged neural activity $\overline{\langle R_i \rangle}$ related to microsaccades during fixation as a function of microsaccadic frequency F, shown in Fig. 2(b). Approximately, the neural activity increases linearly with the frequency F. This result suggests that the new neural response induced by a microsaccade can be regarded as being independent of that by the previous microsaccade, although there exist successive microsaccades. This happens because the neural

activity effectively comes to the baseline due to adaptations before a new microsaccade happens if the frequency F is not very high [Fig. 2(a)]. In the following investigations, we focus on the neural activity induced by an isolated microsaccade after the initial fixation.

In order to study the effect of STD, we compare the response time of the neural activity related to microsaccade in the cascading-adaptation model with that in the absence of STD at the thalamocortical synapses. As shown in Fig. 3(a), the response time (RT) is measured as the time interval from the start of the microsaccade to the response peak after the microsaccade. If the response peak does not occur after the microsaccade, the response time will be marked as 0, which denotes that the microsaccade does not induce an effective response. Here, we study the effects of the microsaccade magnitude M and the time interval (TI) between the onsets of the fixation and the microsaccade. From Figs. 3(b) and 3(d), we can see that there is no effective response induced by microsaccades with too small M or too short TI. When M or TI increases respectively to a certain threshold, the microsaccade can induce an effective neural response (i.e., appearance of a response peak correlated with the microsaccade). Namely, there exists a critical value M^* [(TI)*] so that if $M > M^*$ [TI $>$ (TI)*], then the microsaccade can induce an effective neural response in V1. We note that the critical values M^* and (TI)* in the cascading-adaptation model (i.e., with STD) are both smaller than those without STD (i.e., only the retinal adaptation is present). This observation suggests that the cascading-adaptation model can more easily produce effective response to microsaccades with small magnitude M or short interval TI, when compared to the model without STD. Moreover, we find in Figs. 3(b) and 3(d) that the response time RT related to the microsaccade is shorter in the cascading case than that in the absence of STD. These results indicate that STD in the cascading model can easily and quickly produce effective response to microsaccades.

Importantly, for the effective response to microsaccades, we specifically compare the sustaining time of the response in the cascading-adaptation model with that in the absence of STD. The sustaining time (ST) is regarded as the time interval from response peak to half-height value before decaying to the baseline after the microsaccade [Fig. 3(a)]. Figures 3(c) and 3(e) clearly show that the sustaining time is shorter in the cascading case than that without STD. Thus, STD can reduce the duration of the microsaccade-related response and produce a sharp (fast-depressed) response.

It is plausible to argue whether the effects of the cascading adaptation due to STD could be equivalent to those of a stronger adaption at the retina in the absence of STD. In Figs. 3(b)–3(e), we also give the response time and the sustaining time in a model without STD (i.e., only having retinal adaptation), but with a higher level of the retinal adaptation (by increasing the time scale τ_r of the retinal adaptation, so that the recovery time is longer at the retina). It is found that, the response time and the sustaining time can slightly decrease. That is, the increasing of adaptation level at the retina could slightly compensate for the lack of STD. However, the critical values M^* and (TI)* inducing the effective response are not reduced, but are even increased.

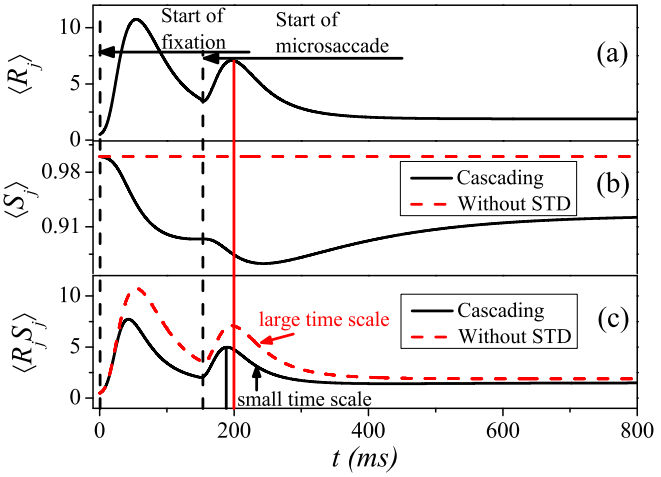

FIG. 4. Comparison of LGN network-averaged firing rate $\langle R_j \rangle$ (a), synaptic strength $\langle S_j \rangle$ (b), and multiplication $\langle R_j S_j \rangle$ (c) induced by a microsaccade in the cascading-adaptation network model and in the absence of STD. Solid vertical lines denote response peaks in (a) and (c), respectively. Here, we use $g = 1.8$, TI $= 150$ ms, and $M = 2.2$.

The above properties of fast and sharp response to microsaccades induced by STD are found to be generic, i.e., robust to parameters (results not shown). Here we study the underlying mechanism of the generic properties. The V1 response results from the input of each thalamocortical synapse from the LGN neuron j, which is proportional to the network-averaged $\langle R_j S_j \rangle$ [13]. So, the LGN response $\langle R_j S_j \rangle$ can be used to reflect V1 response $\langle R_i \rangle$. We compare the $\langle R_j S_j \rangle$ in the cascading-adaptation network model with that in the absence of STD. In Fig. 4, we plot the time evolutions of the network-averaged firing rate $\langle R_j \rangle$, synaptic strength $\langle S_j \rangle$, and the multiplication $\langle R_j S_j \rangle$ from LGN neurons after the fixation and the microsaccade. Clearly, the LGN response $\langle R_j \rangle$ increases to a peak and then decreases after the microsaccade [Fig. 4(a)]. According to Eq. (6), the synaptic strength will exponentially decrease to the approximate steady value $S_j = \frac{1}{f_S + (1-f_S) R_j \tau_S}$ [13], where S_j is roughly inversely proportional to R_j. The time evolution of $\langle S_j \rangle$ is opposite to that of $\langle R_j \rangle$ with time delay determined by Eq. (6) [Fig. 4(b), black solid line]. Clearly, $\langle S_j \rangle$ sequentially decreases when $\langle R_j \rangle$ increases to the response peak after the microsaccade. Thus, the response peak of $\langle R_j S_j \rangle$ appears before the response peak of $\langle R_j \rangle$. Without STD, the synaptic strength S_j is always invariant (here, we let the value to be 1) [Fig. 4(b), red dashed line]. We can get $\langle R_j S_j \rangle = \langle R_j \rangle$ in the absence of STD. Therefore, the appearance of the response peak after the microsaccade in the cascading model with STD is always ahead of that without STD [Fig. 4(c)]. So, STD contributes to faster response to microsaccades.

Next, we focus on the time scales of the decreasing components in the neural response after the microsaccade, in order to study the mechanism of sharp response induced by STD. According to Eqs. (8) and (9), we can theoretically get an exponential decay $\langle R_k \rangle \sim e^{-t/\tau}$ after the response peak with a time scale $\tau \simeq \tau_r / 1 + (1 - f_r) A \tau_r$. So, the LGN response behaves also as an exponential decay $\langle R_j \rangle \sim e^{-t/\tau_1}$

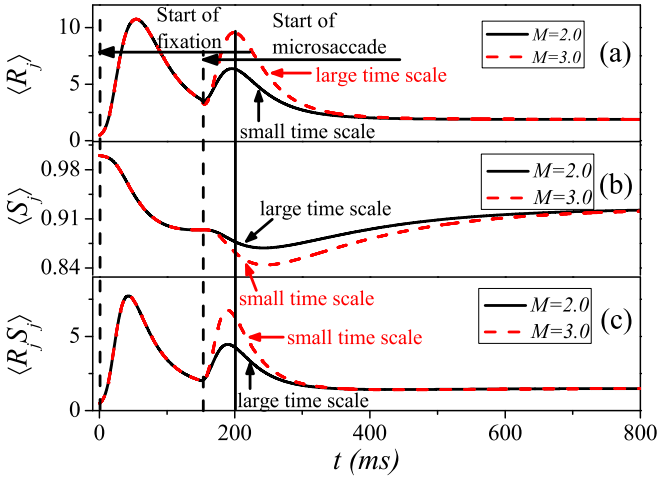

FIG. 5. The same as in Fig. 4, but for the comparison between the two cases with different microsaccade magnitudes ($M = 2$ and 3). The solid vertical line denotes the response peaks in (a). Here, we use $g = 1.8$ and TI = 150 ms.

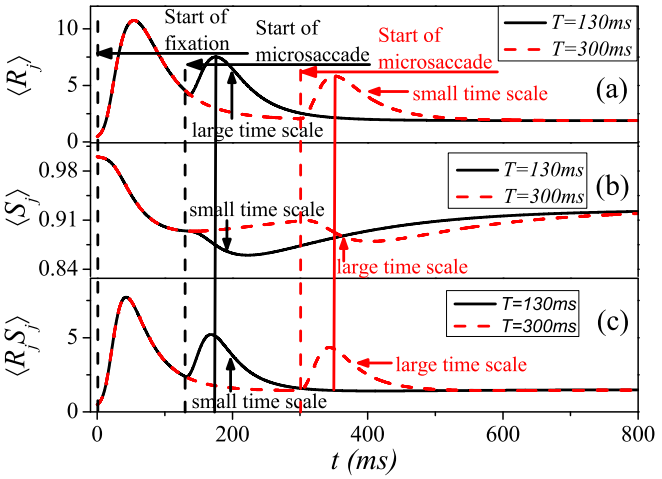

FIG. 6. The same as in Fig. 5, but for the comparison between the two cases with different fixation-microsaccade intervals (TI = 130 ms and 300 ms). Here, $g = 1.8$ and $M = 2.2$ are given.

[Fig. 4(a)] with another time scale τ_1 due to the exponential inputs from retinal responses. According to Eq. (6), $\langle S_j \rangle$ gives another exponential decay $\langle S_j \rangle \sim e^{-t/\tau_2}$ [Fig. 4(b), black solid line] after the microsaccade in the cascading-adaptation network model. Therefore, the multiplication $\langle R_j S_j \rangle$ can be approximately described by $\langle R_j S_j \rangle \sim e^{-(\frac{1}{\tau_1}+\frac{1}{\tau_2})t} = e^{-t/\tau_3}$ with a smaller time scale τ_3 [Fig. 4(c), black solid line], where τ_3 is theoretically smaller than both τ_1 and τ_2. In the absence of STD, $\langle R_j S_j \rangle = \langle R_j \rangle \sim e^{-t/\tau_1}$ exponentially decreases with the larger time scale τ_1 [Fig. 4(c), red dashed line] after the response peak induced by the microsaccade. Since $\tau_3 < \tau_1$, the sustaining time of the response to the microsaccade in the cascading model with STD is shorter than that in the absence of STD.

Moreover, it is noteworthy to see from Fig. 3(c) that the sustaining time in the cascading adaption decreases as M grows. This behavior is contrary to the case where STD is absent. The opposite variations can be explained in Fig. 5. For the larger microsaccadic magnitude M, the response $\langle R_j \rangle$ to the microsaccade can produce a larger peak because of a new large input to LGN by moving the fixated dot over the neurons with less retinal adaptation. The response with a larger peak can last for a longer sustaining time, so the larger peak decreases exponentially with a larger time scale after the response peak [Fig. 5(a)]. In the absence of STD, the time scale of decreasing response $\langle R_j S_j \rangle = \langle R_j \rangle$ for large M is longer than that for small M. Therefore, with the increase of M, the sustaining time of V1 response increases in the model without STD, as shown in Fig. 3(c). When we consider STD at the thalamocortical synapses, $\langle S_j \rangle$ displays the opposite relation of time scales for large and small magnitudes M [Fig. 5(b)], compared with the relation of time scales of $\langle R_j \rangle$ [Fig. 5(a)]. This is because the synaptic strengths $\langle S_j \rangle$ of the newly fixated LGN neurons with the less adaptation for large magnitude M will be more strongly suppressed and decrease immediately and substantially [Fig. 5(b), red dashed line] when the microsaccade appears. The multiplication $\langle R_j S_j \rangle$ can display the same relation of time scales for $\langle S_j \rangle$ for large and small magnitudes M in the cascading model with a strong STD [i.e., the large τ_S and the small f_S in Eq. (6)], as shown in Fig. 5(c). Thus, the sustaining time of V1 response to the microsaccade can decrease with the increasing of M in the presence of strong STD [e.g., the parameters $\tau_S = 200$ ms and $f_S = 0.75$ adopted in this paper, which are fitted by experimental data [13], Fig. 3(c)].

As shown in Fig. 3(e), the sustaining time increases with the increase of TI (within the small region) in the cascading adaptation, while it decreases in the absence of STD. The opposite trends in these two models can be explained in Fig. 6. When the fixation-microsaccade time interval TI is large, the depressed time of the retinal neuron during the fixation is long and the adaptation factor r_k is small in Eq. (9) after the microsaccade. The small r_k produces small response with small time scale for the decrease of $\langle R_j \rangle$ in LGN [Fig. 6(a)]. In the absence of STD, the responses of $\langle R_j S_j \rangle$ and $\langle R_j \rangle$ display the same decrease with small time scale after the response peak

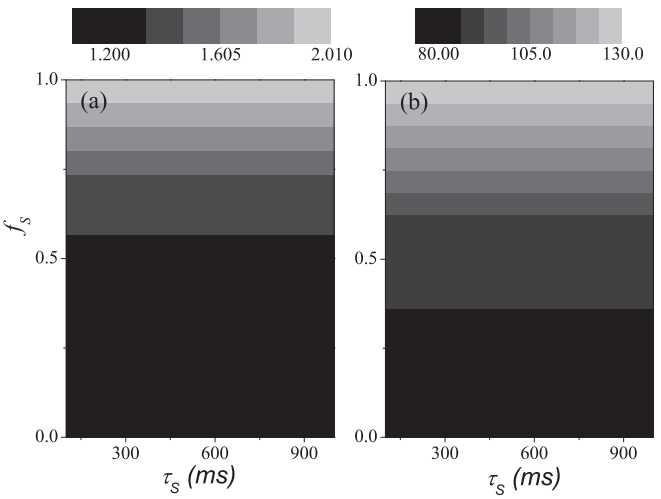

FIG. 7. Phase diagrams of the thresholds M^* (a) and $(TI)^*$ (b) in τ_S-f_S plane. Here, $g = 1.8$, TI = 150 ms (a), and $M = 2.2$ (b).

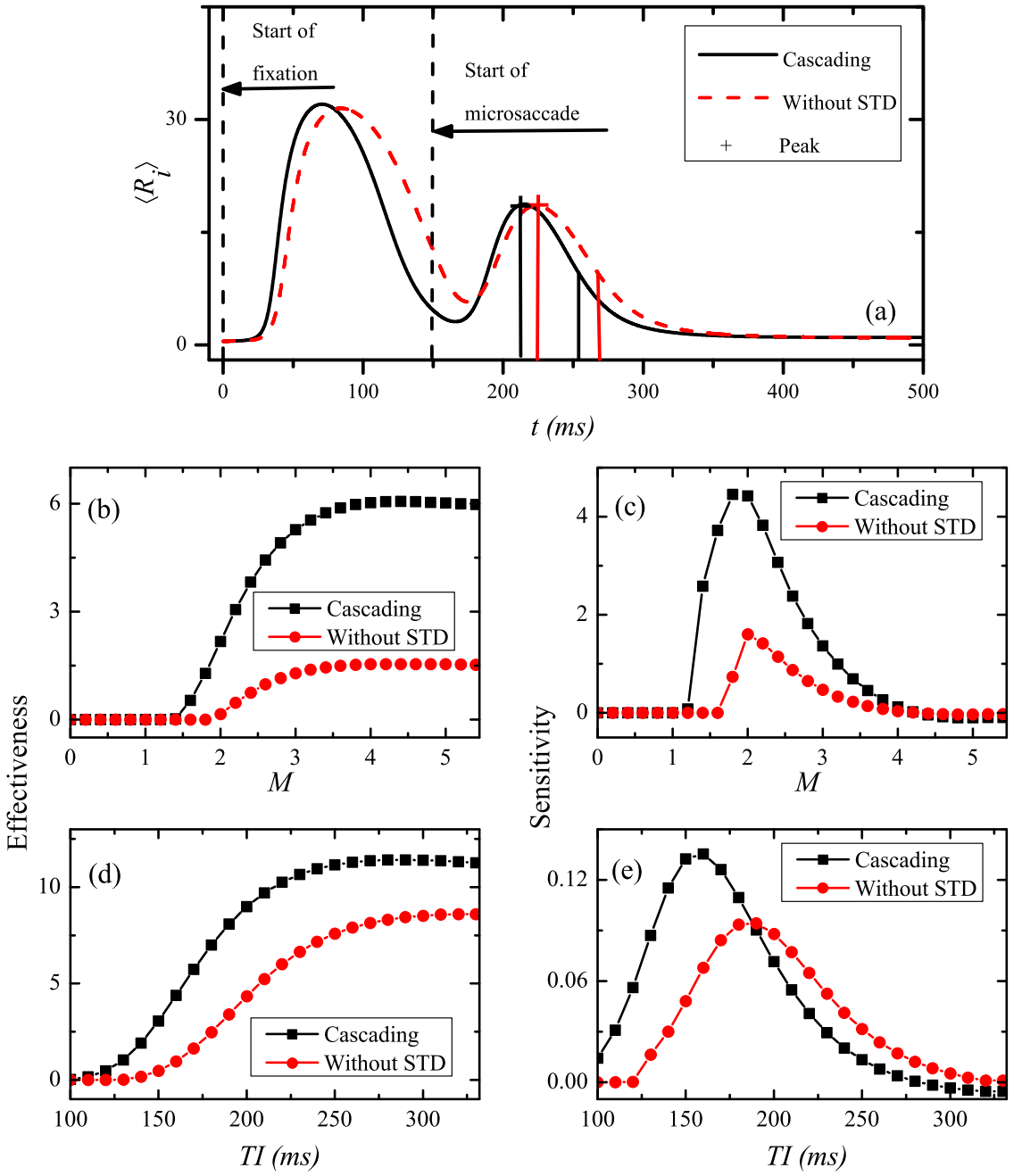

FIG. 8. The same as in Fig. 3, but for the comparison of V1 response effectiveness and sensitivity. Here we adopt $g = 1.8$ from retina to LGN, but $g = 2.8$ from LGN to V1 for the cascading-adaptation model in order to modulate the approximate response peaks after the fixation for eliminating the effect of responsive scale [see (a)]. In (c) and (e), $\Delta(M) = 0.2$ and $\Delta(\mathrm{TI}) = 10$ ms are given, respectively.

for large TI. Therefore, the sustaining time of V1 response $\langle R_i \rangle$ decreases with the increase of TI in the absence of STD [Fig. 3(e)]. With STD, the synaptic strength $\langle S_j \rangle$ in LGN is large at the microsaccade onset time, and decreases with large time scale after the microsaccade for large TI [Fig. 6(b), red dashed line] due to the inverse ratio relation $S_j = \frac{1}{f_S + (1-f_S) R_j \tau_S}$ between S_j and R_j. The multiplication $\langle R_j S_j \rangle$ can display the same relation of time scales of $\langle S_j \rangle$ for large and small intervals TI in the cascading model with a strong STD, as shown in Fig. 6(c). Thus, the sustaining time of V1 response to the microsaccade can increase with TI in the presence of strong STD considered here.

As noted above, the critical values M^* and $(\mathrm{TI})^*$ are smaller in the cascading model with STD [see Figs. 3(b)–3(e)], so STD can more easily evoke the effective response to microsaccades. Here we investigate the dependence of the critical values M^* and $(\mathrm{TI})^*$ on the parameters τ_S and f_S of STD, as shown in Fig. 7. It is found that the critical values M^* and $(\mathrm{TI})^*$ are independent of τ_S for a given f_S. But, they both decrease as f_S becomes smaller (i.e., the adaptation level of STD increases) for a given τ_S. Thus the effective response to microsaccades is sensitive to the variance of STD level by changing f_S. The stronger the STD (by decreasing f_S), the more easily the effective response to the microsaccade will occur.

B. High effectiveness and sensitivity

The above fast-produced and fast-depressed (sharp) response could contribute to providing more resting time for preparing the response to the next microsaccade. So, these results of fast and sharp response induced by STD could imply a highly effective and sensitive response to successive microsaccades or the tiny movements in the visual world. In this section, we investigate in detail the effect of STD on the effectiveness and sensitivity of response to microsaccades in the cascading-adaptation model. The microsaccade-related effectiveness is defined by a relative change of the neural response to the microsaccade, i.e., the difference of the neural responses between the peak after a microsaccade and the baseline before the microsaccade, divided by the baseline. The sensitivity of the effective response to the change of M or TI by an amount $\Delta(M)$ or $\Delta(\mathrm{TI})$ is defined as the change of the effectiveness evoked by a given $\Delta(M)$ or $\Delta(\mathrm{TI})$ divided by $\Delta(M)$ or $\Delta(\mathrm{TI})$. Actually, this definition denotes the slope of effectiveness curve as the function of M or TI if $\Delta(M)$ or $\Delta(\mathrm{TI})$ is infinitesimal. In our simulations, spatial change induced by the microsaccade is assumed to be momentary, and the time interval and microsaccade-microsaccade time interval (i.e., microsaccadic time interval) both denote the time interval between two neighboring fixations. Thus, the fixation-microsaccade time interval TI can be regarded as microsaccadic time interval in the presence of successive microsaccades. Since $\Delta(\mathrm{TI})$ and $\Delta(M)$ respectively denote microsaccadic temporal and spatial variations, the defined sensitivity can be used to reflect the change rate of the neural response effectiveness for detecting microsaccadic spatiotemporal changes.

In Fig. 8, we compare the response effectiveness and sensitivity in the cascading-adaptation model with those in the absence of STD. As shown in Fig. 3(a), the response amplitudes are different in the two models when their parameters are the same. In order to eliminate the effect of the response amplitudes, the amplitudes of the two response peaks in the two cases are modulated to be the same by increasing the synaptic conductance g from LGN to V1 in the cascading-adaptation model, shown in Fig. 8(a). Similarly to Figs. 3(b) and 3(d), there are two critical values M^* and TI^*. When $M > M^*$ or $\mathrm{TI} > \mathrm{TI}^*$, the effective response (i.e., nonzero effectiveness) appears in Fig. 8(b) or 8(d). Obviously, the response effectiveness is larger in the cascading-adaptation model than that in the absence of STD, indicating that STD enhances the response effectiveness.

Particularly, STD greatly increases the sensitivity to small changes, $\Delta(M)$, in the value of microsaccade size M [Fig. 8(c)]. In the cascading model, the sensitivity is approximately two times larger than that in the absence of STD. STD can also enhance the sensitivity to small changes $\Delta(\mathrm{TI})$ at small values of TI [Fig. 8(e)]. But as TI increases to large values, the sensitivity with STD is slightly smaller than that without STD. This is because STD can easily make response effectiveness saturated for large TI [Fig. 8(d)] owing to sharp response with fast decay to baseline [Fig. 8(a)]. These results suggest that STD enhances the effectiveness and sensitivity of the neural responses to microsaccades and therefore improves the detection of microsaccadic spatiotemporal variations.

IV. CONCLUSION AND DISCUSSION

To sum up, we proposed a cascading-adaptation network model including both the retinal adaptation and STD at the thalamocortical synapses. It was found that STD not only can more easily induce the effective response to microsaccades but also can make the response faster and sharper when compared to the case without STD. Moreover, STD can enhance the response effectiveness and sensitivity to microsaccade-generated spatiotemporal changes, which indicates that STD can improve the detection of microsaccades.

In our model, microsaccades are regarded as the relative slight movements of the fixated dot. Actually, both neural processing dynamics as well as the perceptual interpretation of a stimulus can also depend on sensory history (e.g., slight movement of the fixated dot) [44]. Thus, the reported effects of STD on the neural responses to microsaccades can also denote contributions of STD to neural activity related to moving visual stimuli. Therefore, STD can also give rise to fast and sharp response to visual motion. Moreover, it can also enhance the response effectiveness and sensitivity to slight movement of visual stimuli, implying that STD could improve the detection of slight movement of visual objects.

It is noteworthy that changes of the sustaining time as a function of M and of TI in the cascading adaptation and those in the absence of STD display opposite trends [Figs. 3(c) and 3(e)]. The sustaining time of the responsiveness monotonously decreases (increases) with M (TI) (within the region of small values) in the cascading adaptation, while it monotonically increases (decreases) in the absence of STD. Since microsaccades could be required for counteracting visual fading during fixation [1,2], the sustaining time of the neural response induced by microsaccades can reflect the time interval between two consecutive microsaccades. Therefore, according to Fig. 3(c), we could give a behavioral prediction of the relation between microsaccadic magnitudes and intervals in the presence of STD: a smaller micacrosaccdic interval could follow the previous microsaccade with a larger size (in the sense of statistical average). Without STD, the relation however could behave oppositely. Similarly, according to Fig. 3(e) we could also give another behavioral prediction about the relation of two adjacent microsaccadic intervals. STD contributes to a slightly linear positive relation between two adjacent microsaccadic intervals. Namely, if the microsaccadic time interval is large, the next microsacadic time interval could also tend to be large (in the sense of statistical average), and vice versa. However, in the absence of STD the behavioral relation might exhibit an opposite trend. Therefore, the two predictions could be used to experimentally verify the important role of STD in the neural response to microsaccades by finding the evidence for the above relationships.

The STD mode in Eq. (6) is a deterministic description of synapse depression (i.e., the release of synaptic vesicles is deterministic). Recent work has shown that the role of stochasticity in synapses with STD plays an important role in explaining important aspects of V1 responses [45,46]. Since microsaccades are stochastic [1], the interplay between two stochastic dynamics could make the study of successive microsaccades both interesting and challenging by using the stochastic STD model. In the future, further investigations are

expected to explore more dynamical properties induced by successive microsaccades.

Generally, our cascadingadaptation model considers simultaneously retinal adaptation and STD at the thalamocortical synapses in the study of neural activity related to microsaccades, therefore it may provide a starting point for modeling visual processes of microsaccades. Our model can provide a useful tip for the understanding of behavioral properties and functional roles of microsaccades and other types of eye movements in the future.

ACKNOWLEDGMENTS

This work is partially supported by the Hong Kong Baptist University (HKBU) Strategic Development Fund; the NSFC-RGC Joint Research Scheme HKUST/NSFC/12-13/01 (or N_HKUST 606/12), RGC12302914; the National Natural Science Foundation of China under Grants No. 11275027 and No. 11005047; the Natural Science Foundation of Anhui Province under Grant No. 1508085MA04; the Project of Natural Science in Anhui Provincial Colleges and Universities under Grants No. KJ2015ZD33 and KJ2016B006; the Major Project of Outstanding Young Talent Support Program in Anhui Provincial Colleges and Universities under Grant No. gxyqZD2016410; the Young Fund of Huaibei Normal University under Grant No. 2013xqz17; and the Scientific and Technological Activity Foundations for Preferred Overseas Chinese Scholar in the Ministry of Human Resources and Social Security of China and in the Department of Human Resources and Social Security of Anhui Province.

[1] S. Martinez-Conde, S. L. Macknik, X. G. Troncoso, and D. H. Hubel, Trends Neurosci. **32**, 463 (2009).
[2] M. Rolfs, Vision Res. **49**, 2415 (2009).
[3] K. Mergenthaler and R. Engbert, Phys. Rev. Lett. **98**, 138104 (2007).
[4] J.-R. Liang, S. Moshel, A. Z. Zivotofsky, A. Caspi, R. Engbert, R. Kliegl, and S. Havlin, Phys. Rev. E **71**, 031909 (2005).
[5] S. Martinez-Conde, Progr. Brain Res. **154**, 151 (2006).
[6] R. Ditchburn and B. Ginsborg, Nature (London) **170**, 36 (1952).
[7] R. Engbert and K. Mergenthaler, Proc. Natl. Acad. Sci. USA **103**, 7192 (2006).
[8] G.-L. Li, J. Vigh, and H. von Gersdorff, J. Neurosci. **27**, 7377 (2007).
[9] K. Rabl, L. Cadetti, and W. B. Thoreson, J. Neurosci. **26**, 2555 (2006).
[10] K. Y. Wong, F. A. Dunn, and D. M. Berson, Neuron **48**, 1001 (2005).
[11] D. A. Butts, P. O. Kanold, and C. J. A. Shatz, PLoS Biol. **5**, e61 (2007).
[12] C. Sharpe, J. Physiol. (London) **222**, 113 (1972).
[13] L. Abbott, J. Varela, K. Sen, and S. Nelson, Science **275**, 220 (1997).
[14] K. Stratford, K. Tarczy-Hornoch, K. Martin, N. Bannister, and J. Jack, Nature (London) **382**, 258 (1996).
[15] N. Bannister, J. Nelson, and J. Jack, Philos. Trans. R. Soc. London B **357**, 1793 (2002).
[16] C. Boudreau and D. Ferster, J. Neurosci. **25**, 7179 (2005).
[17] M. Carandini, D. J. Heeger, and W. Senn, J. Neurosci. **22**, 10053 (2002).
[18] F. Chance and L. Abbott, Neurocomputing **38**, 141 (2001).
[19] F. S. Chance, S. B. Nelson, and L. F. Abbott, J. Neurosci. **18**, 4785 (1998).
[20] X. Xie and H. S. Seung, Phys. Rev. E **69**, 041909 (2004).
[21] P. H. E. Tiesinga, Phys. Rev. E **69**, 031912 (2004).
[22] J. Karbowski, Phys. Rev. E **61**, 4235 (2000).
[23] A. Levina, J. M. Herrmann, and T. Geisel, Nat. Phys. **3**, 857 (2007).
[24] G. Mongillo, O. Barak, and M. Tsodyks, Science **319**, 1543 (2008).
[25] P. Scott, A. I. Cowan, and C. Stricker, Phys. Rev. E **85**, 041921 (2012).
[26] L. Abbott and W. Regehr, Nature (London) **431**, 796 (2004).
[27] C. Fung, K. Wong, H. Wang, and S. Wu, Neural Comput. **24**, 1147 (2012).
[28] M. Merkel and B. Lindner, Phys. Rev. E **81**, 041921 (2010).
[29] Y. Igarashi, M. Oizumi, and M. Okada, Phys. Rev. E **85**, 016108 (2012).
[30] W.-J. Yuan, O. Dimigen, W. Sommer, and C. Zhou, Front. Comput. Neurosci. **7**, 47 (2013).
[31] J.-F. Zhou, W.-J. Yuan, Z. Zhou, and C. Zhou, Sci. Rep. **6**, 20888 (2016).
[32] J. R. Müller, A. B. Metha, J. Krauskopf, and P. Lennie, Science **285**, 1405 (1999).
[33] J. M. Alonso, W. M. Usrey, and R. C. Reid, J. Neurosci. **21**, 4002 (2001).
[34] M. Tsodyks and C. Gilbert, Nature (London) **431**, 775 (2004).
[35] T. Poggio, M. Fahle, and S. Edelman, Science **256**, 1018 (1992).
[36] D. Ferster and K. Miller, Annu. Rev. Neurosci. **23**, 441 (2000).
[37] P. Seriès, P. Latham, and A. Pouget, Nat. Neurosci. **7**, 1129 (2004).
[38] P. beim Graben C. Zhou, M. Thiel, and J. Kurths, *Lectures in Supercomputational Neuroscience: Dynamics in Complex Brain Networks* (Springer, Berlin, 2007).
[39] L. Abbott and S. Nelson, Nat. Neurosci. **3**, 1178 (2000).
[40] I. Nir, J. M. Harrison, R. Haque, M. J. Low, D. K. Grandy, M. Rubinstein, and P. M. Iuvone, J. Neurosci. **22**, 2063 (2002).
[41] B. Ölveczky, S. Baccus, and M. Meister, Neuron **56**, 689 (2007).
[42] J. Demb, J. Physiol. (London) **586**, 4377 (2008).
[43] K. Donner and S. Hemilä, Vision Res. **47**, 1166 (2007).
[44] V. Willert and J. Eggert, Neurocomputing **74**, 1329 (2011).
[45] R. Moreno-Bote, PLoS Comput. Biol. **10**, e1003522 (2014).
[46] J. de la Rocha, R. Moreno, and N. Parga, Neurocomputing **58**, 313 (2004).